

Journal of
Reinforced Plastics and Composites

Shape memory characteristics of woven glass fibre fabric-reinforced epoxy composite in flexure

Journal:	<i>Journal of Reinforced Plastics and Composites</i>
Manuscript ID:	Draft
Manuscript Type:	Original Article
Date Submitted by the Author:	n/a
Complete List of Authors:	Fejős, Márta; Faculty of Mechanical Engineering, Budapest University of Technology and Economics, Department of Polymer Engineering Romhány, Gabor; Faculty of Mechanical Engineering, Budapest University of Technology and Economics, Department of Polymer Engineering Karger-Kocsis, Jozsef; Faculty of Mechanical Engineering, Budapest University of Technology and Economics, Department of Polymer Engineering
Keyword:	shape memory polymer, epoxy, composite, glass fibre fabric, recovery stress
Abstract:	Shape memory characteristics of a woven glass fibre (GF) fabric reinforced epoxy composite (reinforcement content: 38 vol.%) were assessed in three point bending mode in a dynamic-mechanical analysis device and compared to those of the parent epoxy resin (EP). From unconstrained tests the shape fixity and recovery ratios and the recovery rate, whereas from constrained tests the recovery stress were determined. The shape fixity and recovery rate decreased due to the GF reinforcement which had, however, no effect on the shape recovery. Major benefit of the woven GF fabric was that the recovery stress could be enhanced by two orders of magnitude in comparison to the neat EP. GF reinforcement was accompanied with a substantial decrease in the failure-free flexural deformability of the composite specimen.

SCHOLARONE™
Manuscripts

1
2
3
4
5
6
7
8
9
10
11
12
13
14
15
16
17
18
19
20
21
22
23
24
25
26
27
28
29
30
31
32

SHAPE MEMORY CHARACTERISTICS OF WOVEN GLASS FIBRE FABRIC-
REINFORCED EPOXY COMPOSITE IN FLEXURE

14
15
16
17
18
19
20
21
22
23
24
25
26
27
28
29
30
31
32

M. Fejős¹, G. Romhány¹ and J. Karger-Kocsis^{1,2}

*¹Department of Polymer Engineering, Faculty of Mechanical Engineering, Budapest
University of Technology and Economics, Muegyetem rkp. 3., H-1111 Budapest,
Hungary*

*²MTA–BME Research Group for Composite Science and Technology, Muegyetem rkp.
3., H-1111 Budapest, Hungary*

33
34
35
36
37
38
39
40
41
42
43
44
45
46
47
48
49
50
51
52
53
54
55
56
57
58
59
60

Corresponding author:

Márta Fejős, Department of Polymer Engineering, Faculty of Mechanical Engineering,
Budapest University of Technology and Economics, Muegyetem rkp. 3., Budapest H-
1111, Hungary.

Email: fejos@pt.bme.hu

Submitted to J. Reinf. Plast. Compos., July, 2012

Abstract

Shape memory characteristics of a woven glass fibre (GF) fabric reinforced epoxy composite (reinforcement content: 38 vol.%) were assessed in three point bending mode in a dynamic-mechanical analysis device and compared to those of the parent epoxy resin (EP). From unconstrained tests the shape fixity and recovery ratios and the recovery rate, whereas from constrained tests the recovery stress were determined. The shape fixity and recovery rate decreased due to the GF reinforcement which had, however, no effect on the shape recovery. Major benefit of the woven GF fabric was that the recovery stress could be enhanced by two orders of magnitude in comparison to the neat EP. GF reinforcement was accompanied with a substantial decrease in the failure-free flexural deformability of the composite specimen.

Keywords

shape memory polymer, epoxy, composite, glass fibre fabric, recovery stress

Introduction

A shape memory polymer (SMP) is an actively moving polymer, which recovers its original shape from a previously programmed, temporary shape upon an external stimulus. The temporary shape can be achieved by mechanical loading in presence of the external stimulus (usually temperature) and fixed by removing or changing this stimulus.

Primarily, the external stimulus is the temperature increment, which can be triggered by both direct and indirect (i. e., by applying electric current¹, magnetic field², infrared light³) heating. The shape memory effect is induced, when the SMP reaches a critical temperature, called transformation temperature (T_{trans}). For thermo-responsive amorphous and semicrystalline SMPs the glass transition temperature (T_g) and the melting temperature (T_m) serve as T_{trans} , respectively. For SMPs with T_g as T_{trans} the shape memory effect can be also initiated by “softening” the SMP with an appropriate solvent⁴, because this is associated with T_g depression. Researchers prepared also light-⁵ and water-sensitive⁶ SMPs the working principle of which differs from that of thermo-sensitive SMPs.

SMPs may have many advantages, such as easy processability, low cost, light weight, deformability, biocompatibility, biodegradability, etc. compared to other shape memory materials, like shape memory alloys (SMAs) or shape memory ceramics. However,

1
2
3
4
5
6
7
8 SMPs have some limitations⁷, from which low recovery stress is the most important
9 problem with respect to potential applications. Increasing the low recovery stress (from
10 4-10 MPa to 200-400 MPa) of SMPs is nowadays a major challenge in this field.
11
12

13
14
15
16 Unconstrained recovery measurements are generally used to characterise the shape
17 memory behaviours (shape fixity, shape recovery), but they do not provide data for the
18 recovery stress. Recovery stress can be quantified in fully or partially constrained
19 recovery tests⁸.
20
21
22
23

24
25
26 As Rousseau pinpointed⁷, the recovery stress increases with increasing modulus of the
27 SMP. The easiest way to increase the modulus is making SMP composites⁹. Lan et al.¹⁰
28 and Ivens et al.¹¹ followed this direction by incorporating reinforcing fabrics in styrene
29 based thermosetting SMP resins.
30
31
32
33

34
35 Epoxy based SMPs are covalently crosslinked, amorphous thermosets, whose T_g is the
36 T_{trans} . Conventional epoxy resins (EP) are used as adhesives, coatings, sealants and as
37 matrices in composites for structural parts. While development of conventional EPs
38 targets T_g enhancement¹², the research with shape memory EPs is rather focusing on T_g
39 tailoring for different applications¹³.
40
41
42
43
44
45

46
47 Woven glass fibre fabric is one of the most common reinforcements of EPs.
48 Interestingly, the shape memory properties of woven glass fibre fabric/EP composites
49 have been rarely investigated. Therefore this work was aimed at characterising the
50
51
52
53
54
55
56
57
58
59
60

1
2
3
4
5
6
7
8
9 shape memory characteristics of a glass fibre fabric reinforced EP and comparing to
10 those of the neat EP resin. The specimens were subjected to three-point bending tests in
11 a dynamic mechanical analysis (DMA) device to determine the basic shape memory
12 properties. DMA tests were run in both unconstrained and fully constrained conditions
13 whereby avoiding failure onset in the specimens. The constrained DMA tests served to
14 quantify the recovery stress.
15
16
17
18
19
20
21
22
23

24 **Experimental**

25
26 Glycerol based aliphatic epoxy resin (ipox MR 3012) and cycloaliphatic amine curing
27 agent (ipox MH 3122) were purchased from IpoX Chemicals (Budapest, Hungary).
28 Woven E-glass fabric with an area density of 250 g/m² (E 220, Saint-Gobain Vertex,
29 Litomysl, Czech Republic) was used as reinforcement.
30
31
32
33
34
35

36 The mixture of EP and curing agent with the stoichiometric ratio was introduced in
37 between two glass plates positioned with silicone rubber strips at a distance of 1 mm
38 from one another. Polyethylene foil, smeared with mould release agent (Formula Five,
39 Rexco, Conyers, Georgia, USA) was used to facilitate demoulding. Parallel clamps
40 fastened the glass plates and kept in vertical position. The EP resin was poured in the
41 glass plate assembly from its top (Figure 1).
42
43
44
45
46
47
48
49

50 **Figure 1**

1
2
3
4
5
6
7
8
9 The woven glass fibre fabric reinforced epoxy composite (EPGF4), containing four
10 layers, was prepared by hand lamination. The glass fibre (GF) content of EPGF4 was 38
11 vol.%. Both pure epoxy (EP) and EPGF4 were cured at room temperature for 48 hours
12 and post cured at 80°C for 2 hours.
13
14
15

16
17
18 A Q800 dynamic mechanical analyser (DMA, TA Instruments) was used to determine
19 the storage modulus (E' , MPa) and the loss angle ($\tan\delta$, -) as a function of temperature
20 (T , °C) for the EP and EPGF4. Three-point bending mode was applied with a span
21 length of 20 mm. The width and the thickness of the specimens were approximately 10
22 mm and 1 mm, respectively. The scanning range of temperature was -20...150 °C and a
23 heating rate of 3°C/min and a frequency of 1 Hz were selected. T_g was defined as the
24 offset point of $E'(T)$ and the peak position of $\tan\delta(T)$ and denoted by $T_g^{E'}$ and $T_g^{\tan\delta}$,
25 respectively.
26
27
28
29
30
31
32
33
34
35

36
37 Force-controlled three-point bending tests were conducted at 90°C (deformation
38 temperature, T_d) in the above DMA device. The specimen dimensions and the
39 arrangement were the same as written above. Bending speed was 3N/min. The stress
40 and strain values were calculated according to EN ISO 178:2001.
41
42
43
44
45

46
47 In order to determine the shape memory properties two different measurements were
48 performed in the Q800 DMA device. The unconstrained recovery test was used to
49
50
51
52
53
54
55
56
57
58
59
60

determine the shape fixity ratio, the shape recovery ratio and the speed of recovery. This test contained four steps:

- I. Heating up to $T_d = 90^\circ\text{C}$.
- II. Bending to the required or maximum deformation ε_m (which was 1 % - see later) with a deformation speed of 0.2%/min.
- III. Fixing the temporary shape: cooling to the storage temperature, $T_s = 10^\circ\text{C}$, while keeping the required deformation (by applying force).
- IV/A. Recovering the original shape: heating to $T_d = 90^\circ\text{C}$ while loading the specimen with a minimal force of 0.001 N.

The first three steps were strain-controlled while the fourth one force-controlled. After the third step the specimen relaxed and adapted an $\varepsilon_u \leq \varepsilon_m$ deformation, which is the fixed temporary shape. The ability of fixing of the required temporary shape (ε_m) can be calculated by Equation (1), where R_f is the shape fixity ratio, ε_u is the fixed temporary shape and ε_m is the required temporary shape. In the fourth step the specimen approached its original shape ($\varepsilon_0 = 0$), but it remains some residual deformation, which is the $\varepsilon_p \geq \varepsilon_0$ recovered shape. The ability of recovering the original shape can be computed by Equation (2), where R_r is the shape recovery ratio, ε_m is the required temporary shape and ε_p is the recovered shape, ε_0 is the original shape. Speed of the

1
2
3
4
5
6
7
8
9 recovery is characterised by the recovery rate ($|d\varepsilon/dt|$, %/min, where t is the time)
10
11 measured in step IV/A.

$$R_f = \frac{\varepsilon_u}{\varepsilon_m} 100\% \quad (1)$$

$$R_r = \frac{\varepsilon_m - \varepsilon_p}{\varepsilon_m - \varepsilon_0} 100\% \quad (2)$$

12
13
14
15
16
17
18
19
20
21
22
23
24
25
26
27 The other test was conducted under constrained condition to determine the recovery
28 stress (σ_{rec}). This fully constrained recovery test was carried out in strain-controlled
29 mode. It contains also four steps. The first three steps are identical with those of the
30 unconstrained test (see above). The fourth step was different:
31
32
33
34
35
36

37 IV/B. Heating up to $T_d = 90^\circ\text{C}$ while keeping the required deformation (by applying
38 force).
39
40
41

42 The maximum of stress needed during the second and third step can be defined as the
43 programming stress (σ_{load}). The maximum of stress during the fourth step is the
44 recovery stress (σ_{rec}). It should be noted that the programming conditions (strain rate,
45 heating rate) were the same for the two samples (i.e. EP and EPGF4).
46
47
48
49
50
51
52
53
54
55
56
57
58
59
60

Results and Discussion

The DMA curves (Figure 2) clearly show the effect of the woven GF reinforcement. The GF reinforcement increased prominently the storage modulus, but lowered the difference between the glassy and rubbery moduli, which is proposed to influence the shape memory behaviour¹⁴. Different glass transition temperatures were read from the DMA traces: $T_g^{E'}$ values are 50°C and 44°C whereas the $T_g^{\tan\delta}$ ones 64°C and 59°C for the EP and EPGF4, respectively. The observed shift in the T_g toward lower temperatures in case of the EPGF4 can be traced to the formation of an interphase with higher chain flexibility than the bulk EP. This is obviously an effect of the GF sizing.

Figure 2

For the deformation temperature (T_d) that temperature was selected, where both the samples were in the rubbery state. This was around 90°C, i.e. approximately 30°C higher than T_g . In order to determine the deformability of the samples at T_d flexural tests were conducted.

As expected, the EPGF4 had 2 orders of magnitude larger flexural modulus (3649 MPa compared to 32 MPa for EP), and one order of magnitude larger flexural stress at failure (46 MPa compared to 2 MPa for EP) than the neat EP at 90°C. As a negative effect, the reduction in the flexural strain at failure should be noted. It decreased from 6.6% (EP) to 1.3% (EPGF4). Figure 3 displays the flexural stress-strain curves of the samples.

1
2
3
4
5
6
7
8
9 Failure of the EPGF4 specimen occurred at its compression side, where the glass fabric
10 delaminated and bent in the opposite direction of the bending.
11

12 13 14 **Figure 3**

15
16
17 For shape memory tests an appropriate maximal strain (ϵ_m) level should be chosen. Its
18 value should be as high as possible but without causing any failure in the specimen.
19
20 Based on Figure 3 the $\epsilon_m = 1\%$ was selected.
21
22

23
24 With help of the unconstrained recovery test the basic shape memory characteristics of
25 the samples can be quantified. Figure 4 shows the temperature program, stress and
26 strain values during the test. After deforming the pure EP to ϵ_m and immediate cooling
27 to T_s the stress decreases almost to zero which suggests good shape fixity. The strain
28 shows a small increase during step III, due to thermal contraction. This thermal
29 contraction leads to a shape fixity of 103% for the EP though the theoretical maximum
30 value of shape fixity is 100%.
31
32
33
34
35
36
37
38
39

40 41 **Figure 4**

42
43
44 In case of EPGF4 the stress decreases during cooling, but does not reach zero.
45
46 Therefore, after step III the strain displays a prominent decrease, which implies that its
47 shape fixity is worse than that of the EP. Table 1 lists the determined shape memory
48 properties of the samples.
49
50
51
52
53
54
55
56
57
58
59
60

Table 1

Note that both samples show very good shape recovery ratio (99% each). On the other hand, EPGF4 exhibited a lower maximal recovery rate compared to the neat EP, as Figure 5 shows.

Figure 5

From the three dimensional (3D) temperature-stress-strain plots (Figure 6) the decrease in shape fixity due to the woven GF reinforcement it turns out very clearly. The 3D representation also evidences the stress increment needed to deform the composite specimen. The latter implies an increase in the recovery stress.

Figure 6

Fully constrained recovery tests were aimed at determining the recovery forces (Figure 7 **Error! Reference source not found.**). Recall that the first three steps of this test agree with those of the unconstrained recovery test. Loading (or programming) stress (σ_{load}) and recovery stress (σ_{rec}) are the maximum stress values observed during bending deformation (step II) and during recovery (step IV/B), respectively. Woven GF reinforcement increased σ_{rec} of the EP by two orders of magnitude (Table 1). This is very beneficial for such application of shape memory composites where high recovery forces are needed (e.g. actuators). Note that σ_{rec} and σ_{load} for both EP and EPGF4 are

1
2
3
4
5
6
7
8
9 almost equal. This fact suggests that no crack or other type of failure occurred during
10 the shaping/programming step.
11

12 13 14 **Figure 7** 15

16 17 18 **Conclusion** 19

20 This work was devoted to compare the shape memory characteristics of an epoxy resins
21 (EP) and its composite containing 4 layers woven glass fibre (GF) fabric reinforcement
22 (EPGF4; GF content: 38 vol.%). The shape memory properties were determined in
23 flexure using a dynamic-mechanical analysis (DMA) device working under both
24 unconstrained and constrained conditions. It was found that the shape fixity (from 103
25 to 81%) and recovery rate (from 0.51 to 0.37 %/min) decreased due to the GF
26 reinforcement. By contrast, the reinforcement did not affect the shape recovery and
27 strongly enhanced the recovery stress (from 0.4 to 42 MPa). This was, however,
28 associated with a large decrease in the failure-free flexural deformability of the
29 composite specimen (from 6.6 to 1.2%).
30
31
32
33
34
35
36
37
38
39
40
41
42
43
44
45

46 47 **Funding** 48

49 This work was supported by the Hungarian Research Fund [OTKA NK 83421]; by the
50 scientific programs: "Development of quality-oriented and harmonized R+D+I strategy
51
52
53
54
55
56
57
58
59
60

1
2
3
4
5
6
7
8
9 and functional model at BME" [TÁMOP 4.2.1/B-09/1/KMR-2010-0002]; and „Talent
10 care and cultivation in the scientific workshops of BME" [TÁMOP 4.2.2/B-10/1-2010-
11 0009].
12
13
14

15 16 **References**

- 17
18 1. Lan X, Leng JS, Liu YJ and Du SY. Investigate of electrical conductivity of shape-
19 memory polymer filled with carbon black. *Adv Mater Res* 2008; 47-50: 714–717.
20
21
- 22
23 2. Kumar UN, Kratz K, Behl M and Lendlein A. Shape-memory properties of
24 magnetically active triple-shape nanocomposites based on a grafted polymer network
25 with two crystallizable switching segments. *Express Polymer Letters* 2012; 6: 26–40.
26
27
- 28
29 3. Leng J, Wu X and Liu Y. Infrared light-active shape memory polymer filled with
30 nanocarbon particles. *J. Appl Polym Sci* 2009; 114: 2455–2460.
31
32
- 33
34 4. Huang WM, Yang B, An L, Li C and Chan YS. Water-driven programmable
35 polyurethane shape memory polymer: Demonstration and mechanism. *Appl Phys Lett*
36 2005; 86: 114105/1–114105/3.
37
38
- 39
40 5. Lendlein A, Jiang HY, Junger O and Langer R. Light-induced shape-memory
41 polymers. *Nature* 2005; 434: 879–882.
42
43
44
45
46
47
48
49
50
51
52
53
54
55
56
57
58
59
60

6. Fan K, Huang WM, Wang CC, Ding Z, Zhao Y, Purnawali H, Liew KC and Zheng LX. Water-responsive shape memory hybrid: Design concept and demonstration. *Express Polymer Letters* 2011; 5: 409–416.
7. Rousseau IA. Challenges of shape memory polymers: A review of the progress toward overcoming SMP's limitations. *Polym Eng Sci* 2008; 48: 2075–2089.
8. Lakhera N, Yakacki CM, Nguyen TD and Frick CP. Partially constrained recovery of (meth)acrylate shape-memory polymer networks. *J Appl Polym Sci* 2012; in press, DOI: 10.1002/app.36612.
9. Ware T, Ellson G, Kwasnik A, Drewicz S, Gall K and Voit W. Tough shape-memory polymer–fiber composites. *J Reinf Plast Compos* 2011; 30: 371–380.
10. Lan X, Liu Y, Lv H, Wang X, Leng J and Du S. Fiber reinforced shape-memory polymer composite and its application in a deployable hinge. *Smart Mater Struct* 2009; 18: 024002/1–024002/6.
11. Ivens J, Urbanus M and De Smet C. Shape recovery in a thermoset shape memory polymer and its fabric-reinforced composites. *Express Polymer Letters* 2011; 5: 254–261.

- 1
2
3
4
5
6
7
8
9 12. Yi JW, Um MK, Byun JH, Lee SB and Lee SK. Development of high Tg epoxy
10 resins and mechanical properties of its fiber-reinforced composites. J Appl Polym Sci
11 2012; in press, DOI: 10.1002/app.38040.
12
13
14
15
16 13. Xie T and Rousseau IA. Facile tailoring of thermal transition temperature of epoxy
17 shape memory polymers. Polymer 2009, 50: 1852–1856.
18
19
20
21 14. Ratna D and Karger-Kocsis J. Recent advances in shape memory polymers and
22 composites: A review. J Mater Sci 2008; 43: 254–269.
23
24
25
26
27
28
29
30
31
32
33
34
35
36
37
38
39
40
41
42
43
44
45
46
47
48
49
50
51
52
53
54
55
56
57
58
59
60

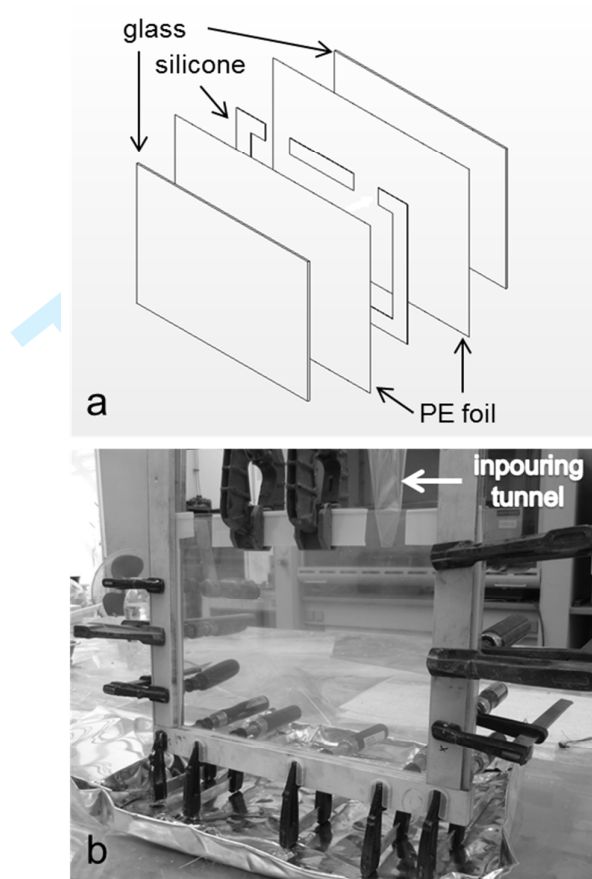


Figure 1. Glass mould for sample preparation of the neat EP:

(a) exploded assembly (b) photograph.

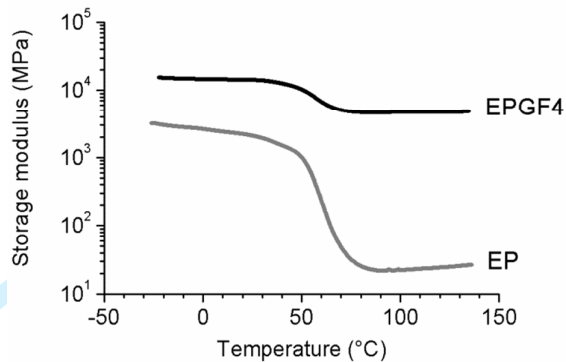


Figure 2. DMA curves of EP and EPGF4.

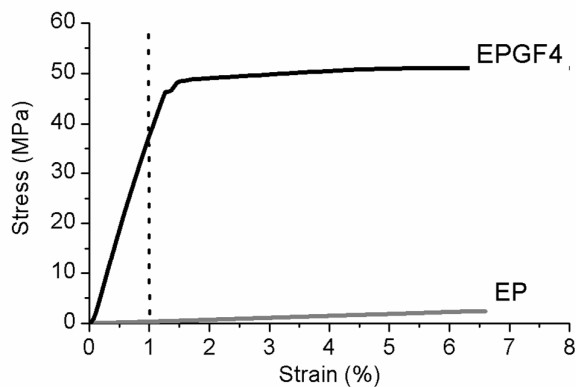


Figure 3. Stress-strain curves of EP and EPGF4 at $T_g + 30^\circ\text{C}$. Dashed line indicates the maximal strain (ϵ_m) applied during the shape memory tests.

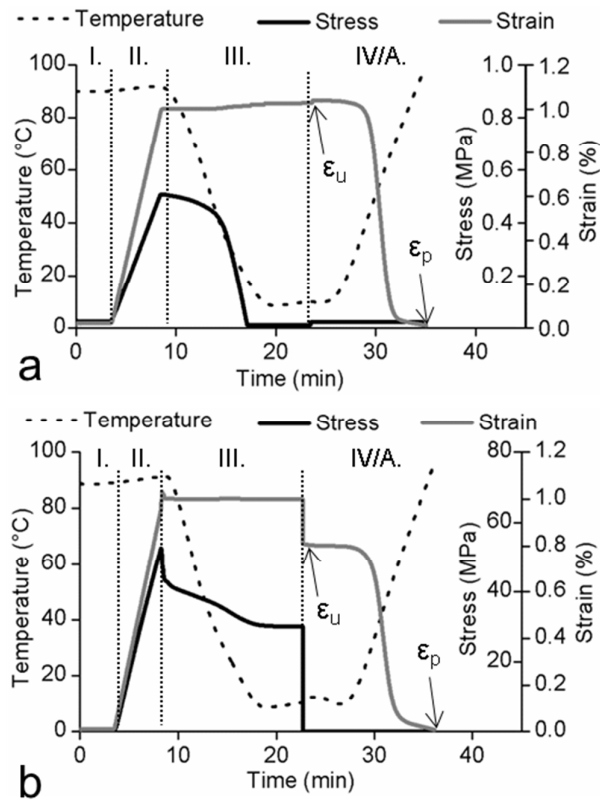


Figure 4. Unconstrained recovery tests on (a) EP and (b) EPGF4.

1
2
3
4
5
6
7
8
9
10
11
12
13
14
15
16
17
18
19
20
21
22
23
24
25
26
27
28
29
30
31
32
33
34
35
36
37
38
39
40
41
42
43
44
45
46
47
48
49
50
51
52
53
54
55
56
57
58
59
60

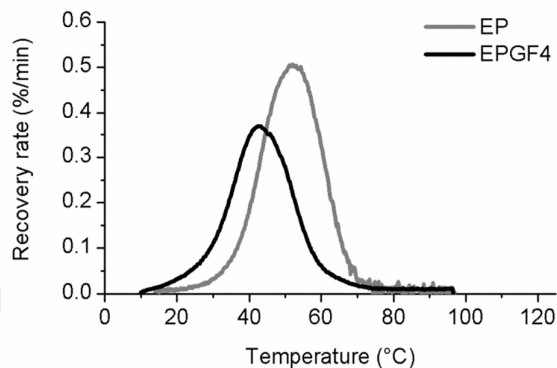


Figure 5. Recovery rate of EP and EPGF4 as a function of temperature.

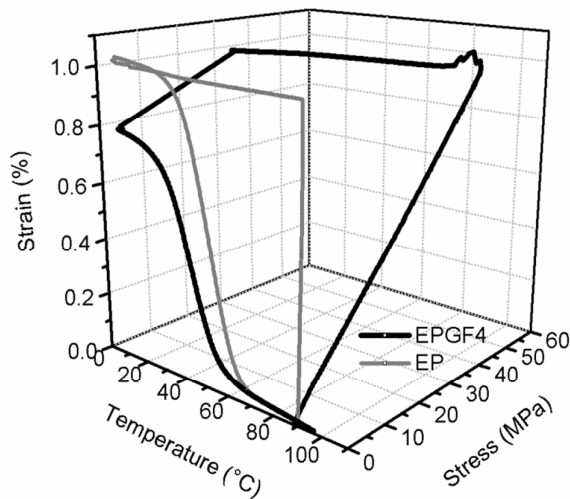


Figure 6. 3D temperature - stress - strain curves of EP and EPGF4.

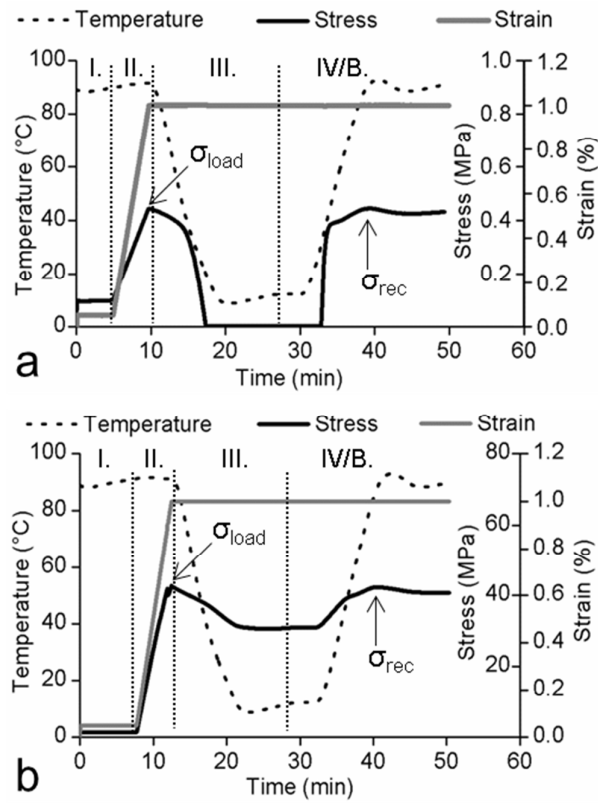


Figure 7. Constrained recovery tests on (a) EP and (b) EPGF4.

1
2
3
4
5
6
7
8
9
10
11
12
13
14
15
16
17
18
19
20
21
22
23
24
25
26
27
28
29
30
31
32
33
34
35
36
37
38
39
40
41
42
43
44
45
46
47
48
49
50
51
52
53
54
55
56
57
58
59
60

Table 1. Shape memory properties of EP and EPGF4.

Properties	EP	EPGF4
ϵ_0 (%)	0	0
ϵ_m (%)	1	1
ϵ_u (%)	1.03	0.81
ϵ_p (%)	0.01	0.01
R_f (%)	103	81
R_r (%)	99	99
$ d\epsilon/dt _{max}$ (%/min)	0.50	0.38
T_r (°C)	51	44
σ_{load} (MPa)	0.44	42.74
σ_{rec} (MPa)	0.44	42.33

For Peer Review